Interleukin-13–Induced Mucous Metaplasia Increases Susceptibility of Human Airway Epithelium to Rhinovirus Infection

Marrah E. Lachowicz-Scroggins[1], Homer A. Boushey[2], Walter E. Finkbeiner[3], and Jonathan H. Widdicombe[1]

[1]Department of Physiology and Membrane Biology, School of Medicine, University of California at Davis, Davis, California; and [2]Cardiovascular Research Institute, Department of Medicine, and [3]Department of Pathology and Laboratory Medicine, School of Medicine, University of California at San Francisco, San Francisco, California

Infection of airway epithelium by rhinovirus is the most common cause of asthma exacerbations. Even in mild asthma, airway epithelium exhibits mucous metaplasia, which increases with increasing severity of the disease. We previously showed that squamous cultures of human airway epithelium manifest rhinoviral infection at levels many times higher than in well-differentiated cultures of a mucociliary phenotype. Here we tested the hypothesis that mucous metaplasia is also associated with increased levels of rhinoviral infection. Mucous metaplasia was induced with IL-13, which doubled the numbers of goblet cells. In both control (mucociliary) and IL-13–treated (mucous metaplastic) cultures, goblet cells were preferentially infected by rhinovirus. IL-13 doubled the numbers of infected cells by increasing the numbers of infected goblet cells. Furthermore, IL-13 increased both the maturity of goblet cells and the probability that a goblet cell would be infected. The infection of cells other than goblet cells was unaltered by IL-13. Treatment with IL-13 did not alter the levels of rhinovirus receptor ICAM-1, nor did the proliferative effects of IL-13 enhance infection, because rhinovirus did not colocalize with dividing cells. However, the induction of mucous metaplasia caused changes in the apical membrane structure, notably a marked decrease in overall ciliation, and an increase in the overall flatness of the apical surface. We conclude that mucous metaplasia in asthma increases the susceptibility of airway epithelium to infection by rhinovirus because of changes in the overall architecture of the apical surface.

Keywords: asthma; interleukin-13; rhinovirus; respiratory tract infection; goblet cells

Bronchial responsiveness to viral respiratory infections is heightened in asthma, and most exacerbations of asthma are associated with such infections (1). Rhinovirus is responsible for more than half of all respiratory-tract infections, and is generally thought to be the most common cause of asthma exacerbations (2–5). Rhinovirus infects the airway epithelium, and the airway epithelium is abnormal in asthma. Although evidence for increased epithelial cell exfoliation exists (6), the best-documented epithelial change, even in mild asthma, is mucous metaplasia (7, 8). We previously showed that the degree of viral infection depends on the type of differentiation of human airway epithelial cell cultures. Specifically, after exposure to the same multiplicity of infection (MOI) of rhinovirus, squamous-cell cultures produced ~100 times as much virus as cultures of healthy mucociliary phenotype (9). We therefore hypothesized that the mucous metaplasia seen in asthma also makes the epithelium more susceptible to viral infection. To test this hypothesis, we used IL-13 to induce mucous metaplasia in cultures of human airway epithelial cells. We then compared the levels of rhinovirus infection in metaplastic cells and cells of a normal mucociliary phenotype.

CLINICAL RELEVANCE

Our studies show that mucous metaplasia increases the susceptibility of the airway epithelium to rhinovirus infection because of a loss of apical membrane complexity. We induced mucous metaplasia with IL-13, which may also be largely responsible for the mucous metaplasia of airway epithelium in asthma. Therefore, in vivo, a blockade of IL-13 may inhibit not only the mucous metaplasia often associated with asthma, but in so doing may also reduce the frequency and severity of asthma exacerbations induced by rhinovirus infection.

MATERIALS AND METHODS

Human Tissues and Cell Culture

Eighteen normal, nondiseased whole tracheas were provided by the National Disease Research Interchange (Philadelphia, PA) within 24 hours of autopsy or surgical resections, through its Human Tissues and Organs for Research Program. Tracheal primary cultures were obtained as previously described (10). In brief, strips of epithelium were removed from underlying tissue and treated with protease overnight. Cells were expanded in a 25–75-cm^2 Corning cell culture treated flasks (Costar, Corning, NY). When cells reached 80% confluence, they were harvested and plated in plating medium at 0.5×10^6 cells/cm^2 on 1.13-cm^2 Transwell polycarbonate inserts in a 12-well cluster (catalogue no. 3401; Costar). To achieve mucociliary differentiation, cells were maintained in a 1:1 mixture of Dulbecco's MEM and Ham's F-12 medium (DME/F12), supplemented with 2% Ultroser G, penicillin, streptomycin, amphotericin B, and gentamycin, and kept at an air–liquid interface (ALI). Squamous-cell cultures were generated by immersion feeding with DME/F12 supplemented with 5% FCS. The medium was replaced every 2 days. Our methods are described in full elsewhere (11, 12). The use of human tissues was approved by the Office of Research at the University of California at Davis, the Committee on Human Research at the University of California at San Francisco, and the Institutional Review Board at each university.

(*Received in original form July 6, 2009 and in final form December 23, 2009*)

This work was supported in part by a Research Grant from GlaxoSmithKline (Philadelphia, PA) by grant 5R01HL080414–04 from the National Heart, Lung, and Blood Institute and a gift from Pam Fair and Glen Sullivan. Confocal microscopy for this investigation was performed in a facility constructed with support from Research Facilities Improvement Program Grants C06 RR17348–01 and C06 RR12088–01 from the National Center for Research Resources, National Institutes of Health.

Correspondence and requests for reprints should be addressed to Jonathan H. Widdicombe, D. Phil., Department of Physiology and Membrane Biology, School of Medicine, University of California at Davis, One Shields Avenue, Davis, CA 95616-8643. E-mail: jhwiddicombe@ucdavis.edu

This article has an online supplement, which is accessible from this issue's table of contents at www.atsjournals.org

Am J Respir Cell Mol Biol Vol 43. pp 652–661, 2010
Originally Published in Press as DOI: 20.1165/rcmb.2009-0244OC on January 15, 2010
Internet address: www.atsjournals.org

Virus Cultures and Titration

Rhinovirus serotype 16 (a gift from Shigeo Yagi, Viral and Rickettsial Disease Laboratory, California Department of Health Services, Richmond CA) was originally obtained from the University of Wisconsin, and had been passaged twice in WI-38 cells. At the Viral and Rickettsial Disease Laboratory, it was passaged three more times through human fetal diploid lung (HFDL) cells, which were grown in roller bottles in Eagle's MEM in Hank's F-12 medium with 10% FBS. Just before inoculation, cells were washed with Eagle's MEM in Hank's F-12 medium without FBS. When the cytopathic effect reached 75–100%, the roller bottles were subjected to three freeze–thaw cycles, and the supernatant was spun at low speed to dispose of cellular debris. The supernatant was collected and frozen at −70°C until use. The concentration of virus in the supernatant was $10^{6.8}$ median tissue culture infective dose ($TCID_{50}$)/ml, as determined using HFDL.

Transepithelial Resistance

Measurements of transepithelial electrical resistance (R_{te}) and transepithelial potential difference (V_{te}) were performed every 2 days immediately before routine media changes. The mucosal surface was covered with PBS (500 μl), and measurements were performed with a "chopstick" voltmeter (Millicell ERS; Millipore Products, Bedford, MA). The PBS solution was immediately removed after measurements were completed. Cell sheets were used only if the R_{te} was greater than 500 Ω × cm^2 and the range of R_{te} of the 12 sheets in the cluster was no more than 200 Ω × cm^2.

Experimental Protocol

Cells became electrically tight (i.e., achieved an acceptable resistance of >500 Ω × cm^2) after 3–5 days in culture. Because cells require ~3–4 weeks in culture to develop maximal mucociliary differentiation (12, 13), we waited a further 14 days before adding IL-13. Based on the literature (14–16) and our own preliminary studies, we induced mucous metaplasia by exposing cultures to 10 ng/ml recombinant human IL-13 for 7 days. Thus, unless otherwise stated, all cells were studied exactly 21 days after becoming electrically tight, i.e., ~24–26 days after plating. Control cells from the same cultures received vehicle alone. After the addition of IL-13, media changes and measurement of R_{te} and V_{te} were performed daily in both treated and control cells. The 500-μl aliquots of apical PBS used to make the electrical measurements were retained for analyses of mucin content. After 7 days of IL-13 treatment, treated and control cells were inoculated with 100 μl of 10^5 $TCID_{50}$/ml of human rhinovirus 16 (RV-16) in PBS on the mucosal surface, and incubated at 37°C for 1 hour. The apical viral suspension was then collected, and "chopstick" voltmeter measurements were obtained. Next, the apical surface was washed three times with 500 μl of PBS, and the final rinse was collected. Basolateral media were then changed. Twenty-four hours after the end of the inoculation period, "chopstick" voltmeter measurements were again acquired, and apical-surface washes and basolateral media samples were collected. Some cell sheets were fixed in 4% paraformaldehyde in phosphate-buffered solution for later structural analyses. Others were placed in 1% SDS buffer with 1:20 protease inhibitor (Broad-Spectrum b2 m; Sigma-Aldrich, St. Louis, MO) for later analyses of cell lysates.

Mucin ELISA

Apical washes from cell lysates were analyzed for total mucin content, using the 17B1/17Q2 mucin ELISA, as described previously (17). A standard curve was generated using known concentrations of lyophilized human mucus (a gift of Dr. Reen Wu, University of California at Davis, Davis, California). Mucin levels were normalized to total cell protein determined with bicinchoninic acid, using BSA as a standard.

Immunofluorescence

Cell sheets and underlying filters were cut from plastic inserts and fixed in 10% neutral buffered formalin for 1 hour before undergoing immunofluorescence. For RV-16 immunofluorescence, cell sheets were placed in a water bath heated to 95°C in 0.01 M sodium citrate buffer for 30 minutes, and then cooled to room temperature for antigen retrieval. Antigen retrieval was used to break protein cross-links formed by formalin fixation, to uncover antigenic sites for the primary antibody. When RV-16 immunofluorescence was combined with the detection of other antigens using identical species–derived primary antibodies, antigen retrieval was applied as described (18). Filters were permeablized in chilled (−20°C) methanol for 10 minutes, followed by three washes for 5 minutes each in TBS. Filters were blocked in a solution of 5% normal goat serum with 1% IgG-free BSA in Tris-buffered saline (TBS) for 1 hour on an orbital shaker (at 70 rpm). After blocking, filters were washed once with TBS for 5 minutes. A solution of mouse anti–RV-16 pool-1 (a gift of Dr. A.G. Mosser, University of Wisconsin, Madison, WI), which binds to the VP2 and VP0 capsid proteins of RV-16 (19), was made in 1% IgG-free BSA in TBS at a final concentration of 1:5,000. Filters were incubated in 150 μl of the solution in the dark overnight at 4°C. After incubation, filters were washed three times for 5 minutes each in TBS buffer with 0.1% Tween-20 (TBS-T). Filters were then incubated with a solution of secondary goat anti-mouse Cy3 antibody in 1% IgG-free BSA made in TBS at a final concentration of 1:200 for 30 minutes on an orbital shaker (at 70 rpm). Filters were then washed three times in TBS-T buffer for 5 minutes each, followed by one wash in TBS buffer for 5 minutes.

Staining with mouse anti-human B6E8, an antibody specific for airway goblet cells (10, 20), rabbit anti-human Ki-67 (clone SP6; Abcam, Cambridge, MA), mouse anti-human MUC5AC (clone 45M1; Santa Cruz Biotechnology, Santa Cruz, CA), rabbit anti-human centrin-1 (C7736; Sigma-Aldrich), which localizes to mature centrioles and basal bodies in ciliated cells (21), and rabbit polyclonal anti-human ICAM-1 (clone H-108; Santa Cruz Biotechnology) was performed under the same conditions as for RV-16, with the exclusion of the first heat antigen retrieval step, unless costaining for RV-16 was involved.

All tissues processed for immunofluorescence were treated with Yo-Pro-1 (Invitrogen, Carlsbad, CA) DNA stain to view nuclei, and were mounted on a slide with an anti-fade solution. For quantification, cell sheets were imaged on Zeiss confocal microscope model L510 Carl Zeiss Microimaging (Jena, Germany). Z-stacks (1 μm between scans) were taken of each field, and the number and average size of nuclei were counted using ImageJ Image Processing and Analysis Software in Java (http://rsbweb.nih.gov/ij/), with an x–y field size of 230 × 230 μm or 320 × 320 μm. The number of RV-16–positive cells was also counted in each stack. Data for each experiment were obtained from three different tracheas, with four randomly selected fields from each of 2–3 cell sheets per culture.

Histology

Cell sheets were cut from plastic inserts before fixing for 1 hour in 10% neutral buffered formalin before routine tissue processing, and were embedded in paraffin. Five-micron sections were stained with mucicarmine and examined with a light microscope equipped with a digital camera. Fluorescent periodic acid Schiff (FPAS) staining was performed with acriflavine HCl, and nuclei were stained with Yo-Pro-1 (22).

Scanning Electron Microscopy

Scanning electron microscopy was performed using standard protocols described previously (23). Apical membrane areas were measured using the Freehand Tool from the ImageJ software toolbar (http://rsb.info.nih.gov/ij/docs/tools.html).

Immunoblotting

Western blot analysis for RV-16 was performed using an 8–18% gradient gel, according to standard blotting protocols described previously, using mouse anti–RV-16 pool-1 (19). Western blot analyses for centrin-1 clone N-15 (Santa Cruz Biotechnology) and ICAM-1 clone H-108 (Santa Cruz Biotechnology) were performed on the same blot in a 10–20% gradient gel. Pooled treated or control cell lysates were made from individual experiments, and 40 μg/ml of total protein from each sample were added per lane. Blots were viewed by chemiluminescence on a Fujifilm LAS-4000 series (GE Healthcare Lifesciences, Piscataway, NJ). Background was subtracted from the images, and after thresholding and binary conversion, the intensity of each band was recorded and expressed as arbitrary units (AUs) of pixel density, using Multi Gauge software (GE Healthcare Lifesciences). Levels of all proteins were normalized to β-actin, determined using mouse anti-β-actin (Sigma-Aldrich). Protein levels were then calculated as $100 \times (AU_{protein} - AU_{background})/(AU_{\beta\text{-actin}} - AU_{background})$, where "protein"

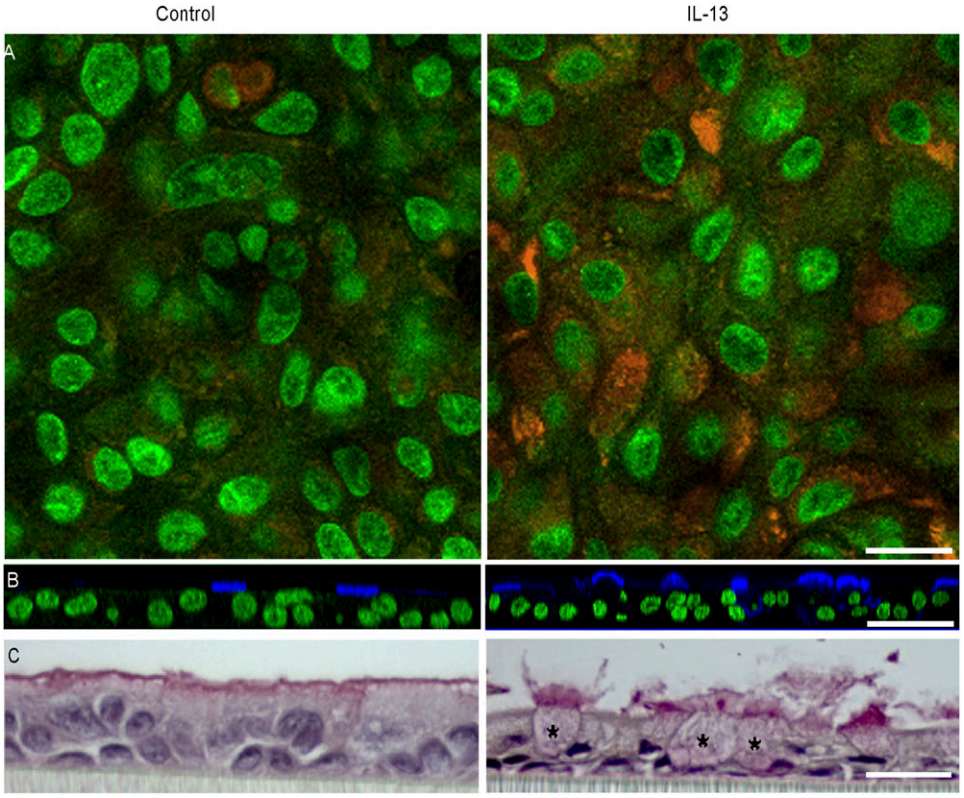

Figure 1. Induction of mucous metaplasia by IL-13. (*A*) Detection of mucus with fluorescent periodic acid Schiff (*orange*). Focal plane, ~5 μm below apical membrane; nuclei are *green*. (*B*) Representative staining of goblet cells with monoclonal antibody B6E8 (*blue*). Nuclei are stained *green* with Yo-Pro-1. (*C*) Light microscopy with mucicarmine staining. Distended cell bodies of several goblet cells are marked by *asterisks*. Several more lie predominantly outside the plane of the section, but all can be identified by the mucus they release. Each pair of images was from cell sheets derived from the same trachea. *Scale bars* = 25 μm (*A*), 50 μm (*B*), and 20 μm (*C*).

refers to AUs obtained for RV-16 viral proteins VP_2 and VP_0, centrin-1, or ICAM-1. "β-actin" refers to AUs obtained for the β-actin standard, and "background" refers to the background AUs obtained from the blot.

Statistical Analysis

Statistically significant differences between means were determined using the Student paired *t* test, with $P < 0.05$ considered statistically significant.

RESULTS

Induction of Mucous Metaplasia

Unless otherwise indicated, all cells were studied 21 days after becoming electrically tight, corresponding to 24–26 days after plating. Moreover, exposure to IL-13 was invariably for 7 days (Days 14–21 after becoming electrically tight) at 10 ng/ml.

IL-13 did not alter the total cell protein levels (592 ± 34 μg/cm^2 for control cells, and 546 ± 36 μg/cm^2 for treated cells). Nor did IL-13 cause a statistically significant change in the total number of cells, with control cultures having an average of 1,280 ± 60 cells per field (of 230 × 230 μm), compared with 1,190 ± 80 cells per field in IL-13–treated cultures. However, control cell sheets had an R_{te} of 1,536 ± 93 versus 966 ± 86 Ω × cm^2 for IL-13–treated cell sheets, a statistically significant difference. Mucin levels secreted at the apical surface were determined from the mucous content of 500-μl aliquots of PBS that were used in performing electrical measurements. In all cultures, the mucous contents increased as cells matured. However, in cells treated with IL-13, mucin content of the bathing medium was significantly elevated, with the highest level seen on Day 7 of treatment, when the total amount of apical mucin was 62.6 ± 2.2 ng, compared with 15.4 ± 2.3 ng in untreated cell sheets ($P < 0.05$). IL-13 induced an increase in numbers of mucous cells, as revealed by staining with FPAS (Figure 1A), staining with antibody B6E8 (Figure 1B), or conventional light microscopy procedures (Figure 1C). Staining with B6E8 or with the mucin 5AC clone 45M1 showed precise colocalizion of the two antibodies (Figure 2), a result predicted by our earlier demonstrations that B6E8 is specific for the mucous granules of airway epithelial goblet cells (10, 20). As measured with B6E8, numbers of goblet cells increased significantly after treatment with IL-13, nearly doubling either in absolute terms or as a percentage of the total cell number (Table 1). The numbers of goblet cells determined with MUC5AC clone 45M1 were not statistically different from those determined with B6E8. Further, the use of MUC5AC clone 45M1 also revealed a significant, ~2-fold increase in goblet-cell numbers induced by IL-13 (as described in the online supplement).

Figure 2. Colocalization of antibodies MUC5AC and B6E8. Panels, left to right: B6E8, MUC5AC and colocalization of both. *Scale bar* = 10 μm.

Exposure to IL-13 also produced a decrease in the number of ciliated cells, as determined by scanning electron microscopy or Western blotting for centrin. Scanning electron microscopy (Figure 3A) showed fewer ciliated cells per unit area of apical surface after IL-13 treatment (19 ± 5 per cm^2 versus 48 ± 6 per cm^2 in untreated control cells). Thus, whereas nonciliated membranes accounted for 27.43% ± 5.48% of the total apical membrane area in mucociliary cultures, this figure increased significantly to 63.60% ± 5.20% in mucous cultures. In agreement with the results of others (16, 24, 25), we also found that cilia were reduced in size after treatment with IL-13.

A loss of cilia upon treatment with IL-13 was also evident from centrin-1 staining (Figure 3B). Western blotting was used to quantify this loss of centrin (Figure 3C). Control cell sheets had an average level of centrin-1 of 0.92 ± 0.23 AUs versus 0.45 ± 0.17 AUs for IL-13–treated cell sheets ($P < 0.05$; paired t test), a significant difference between the two conditions (Figure 3D).

Effects of IL-13 on Rhinovirus Infection

In preliminary experiments, we compared patterns of infection in squamous, mucociliary, and mucous cultures, as revealed by immunocytochemical staining for RV-16. We found no signal in cultures unexposed to virus (Figure 4A). However, after infection, 49% ± 5% of cells in squamous cultures were positive for rhinovirus, and in any given infected cell, multiple foci of infection occurred, averaging ~8 per cell, and ranging as high as 20 (Figure 4B). By contrast, in mucociliary cultures, 1.6% ± 0.09% of cells were infected, and numbers of foci of infection were almost always one per cell, and never more than three (Figure 4C). These results are consistent with our previous studies indicating that squamous cultures of human airway epithelium show levels of viral infection (measured from infectious particles released and levels of viral RNA in cell lysates) ~100-fold greater than those of mucociliary cultures derived from the same tracheas (9). After treatment of mucociliary cultures with IL-13, numbers of rhinovirus-infected cells increased by ~2.5-fold (Figure 4D). Similar to control cells exposed to virus, generally only one focus of infection per cell was evident. The focal planes depicted in Figure 4 were from the middles of cells sheets, where virus was present as discrete foci, usually in the perinuclear region.

Next we performed a quantitative comparison of mucous and mucociliary cultures in terms of numbers of goblet cells and numbers of cells infected with rhinovirus. Representative confocal micrographs from these studies are shown in Figure 4, and the quantitative data are summarized in Figure 2. The confocal images are shown for focal planes either through the center of the cell sheet or just below the apical membrane. This is because the cell sheets consist of several layers, and most cells in the lower layers (corresponding to basal cells of native epithelium) have no contact with the lumen. Thus, levels of virus decline progressively as the focal plane moves deeper into the cell sheet. Changes also occur in the pattern of staining. Near the apical membrane, virus is often associated with mucus and shows a diffuse staining pattern. Nearer the center of the cell sheet, virus is found in discrete perinuclear foci.

In both control and treated cells, rhinovirus preferentially infected goblet cells. Thus, in control cell sheets, ~55% of infected cells were identified as goblet cells by immunocytochemistry (Table 2 and Figures 5A–5C), although goblet cells comprised only 8% of the total (Table 1 and Figures 5A–5C). In IL-13–treated cell sheets, goblet cells comprised 18% of the total cells (Table 1 and Figures 5D–5F) and 76% of infected cells (Table 2 and Figures 5D–5F). The increase in numbers of infected cells induced by IL-13 (171 per field) was almost exactly the same as the increase in the numbers of infected goblet cells (154 per field). The numbers of cells that were infected but did not stain for mucus were not significantly altered by IL-13 treatment (Table 2). Thus, the increase in levels of infection induced by IL-13 was largely attributable to the increase in numbers of goblet cells. However, whereas IL-13 increased total numbers of goblet cells by 91%, it increased the numbers of infected goblet cells by 261%. Thus, IL-13 increased the likelihood that goblet cells would be infected: 17% of goblet cells were infected in control cell sheets, and 32% were infected after treatment with IL-13. The predominant colocalization of mucus and virus in cell sheets treated with IL-13 is illustrated in Figure 5F.

TABLE 1. TOTAL NUMBER OF GOBLET CELLS PER FIELD (OF 320 × 320 μM)

	Control Cells	IL-13
Total number of cells	4,227 ± 310	3,767 ± 113
Total number of goblet cells	352 ± 9	674 ± 17*

Data were collected from six mature cell sheets grown at an air–liquid interface from two different tracheas with four randomly selected fields from each sheet. Goblet cells were detected with antibody B6E8.

* Significantly different from control cells.

To confirm that treatment with IL-13 increased the level of viral infection of mucociliary cultures, we performed Western blotting for capsid protein. As shown in Figure 6, IL-13 treatment significantly increased levels of both provirions, as measured by VP_0, and mature infectious virions, as measured by VP_2. The former increased by 152%, and the latter by 165%, in good agreement with the 155% increase in numbers of infected cells revealed by immunocytochemistry.

The treatment of squamous cultures with IL-13 (using the same exposure regimen as for mucociliary cultures) altered neither the number of cells infected with rhinovirus (45% ± 2%, versus 49% ± 5% in untreated cells) nor the number of foci of infection per cell (data not shown). Furthermore, IL-13 did not induce the formation of mucins in squamous cultures, as determined by FPAS, staining with mAb B6E8, or conventional light microscopy.

Possible Modes of Action of IL-13 on Viral Infection

Two hypotheses initially arose to explain why the mucous metaplasia induced by IL-13 was associated with increased levels of rhinovirus infection. First, levels of ICAM-1, the major receptor for RV-16, may have increased. Second, rhinovirus may preferentially infect dividing cells, and the numbers of these cells might increase in the metaplastic state.

To test the first hypothesis, we localized ICAM-1 by immunocytochemistry, and found the strongest signal by far to come from the apical membrane in both mucociliary and mucous cultures (Figures 7A and 7B). Interestingly, considerable variation occurred in the levels of apical membrane ICAM-1 from cell to cell, and no correlation was evident between levels of apical ICAM-1 and levels of apical mucus. On the other hand, no difference was apparent in ICAM-1 distribution or staining intensity in the apical membranes of the two phenotypes. Furthermore, Western blotting revealed no difference in total levels of ICAM-1 in paired mucous and mucociliary samples from six different cultures (Figures 7C and 7D). Squamous cultures had ~4 times as much ICAM-1 as either mucous or mucociliary cultures.

To test the second hypothesis, that the increase in levels of viral infection induced by IL-13 was attributable to an increase in the numbers of cycling cells, we stained for Ki-67, a nuclear protein found in cells in all phases (G_1, S, G_2, and M) of the

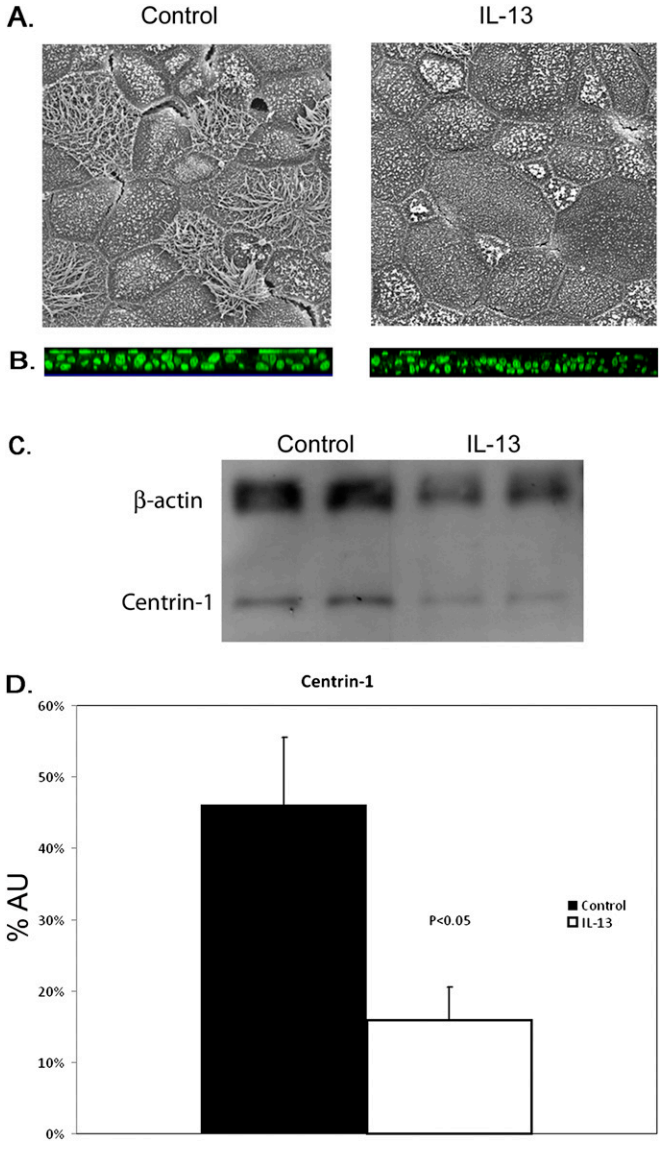

Figure 3. Decreased ciliogenesis induced by IL-13 treatment. (*A*) Scanning electron micrographs of apical surface of mature cell sheets. Large apical surface area and a decrease in ciliated cells are evident after treatment with IL-13. (*B*) Immunofluorescence of centrin-1. Cilia are evident at the apical surface of cell sheets (*green*). (*C*) Quantification of cilia in airway epithelial cells by centrin-1 Western blot. IL-13–treated cell sheets have lower concentration of centrin-1 protein, when normalized to β-actin levels. (*D*) Pooled data from three experiments. Centrin-1 is detected at ~2-fold higher level in cell lysates from control cell sheets. AU, arbitrary units as a measure of pixel density. Centrin-1 levels were normalized to β-actin. Means ± SE for 2–3 cells sheets for three cultures.

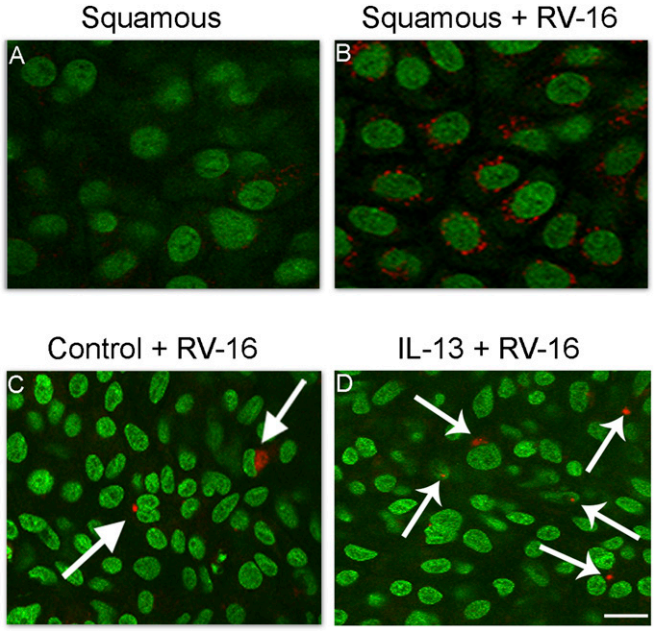

Figure 4. Detection of rhinovirus infection of airway epithelial cells by rhinovirus (*RV*)-16 immunohistochemistry (nuclei, *green*, using Yo-Pro-1; RV-16, *red*). (*A*) Squamous-cell cultures not receiving virus. (*B*) Squamous cultures exposed to RV-16. (*C*) Mucociliary cultures exposed to virus demonstrate occasional perinuclear staining of infectious particles (*arrows*). (*D*) IL-13–treated cells exposed to virus. Cell sheets are from the same tissue. *Scale bar* = 10 μm.

growth cycle, but not in cells during G_0. Preliminary studies were performed to determine the levels of cycling with Ki-67 staining at different times after plating. At 24 hours after plating, ~30% of cells were cycling. At 48 hours, ~ 80% of cells were cycling, and mitotic figures were occasionally seen. By 5 days in culture, however, the cells were confluent and polarized (high transepithelial resistance), individual cells and nuclei were much smaller than at 24 or 48 hours, and cells in the growth phase comprised only ~5% of the total. By 3 weeks, only 1–2% of cells stained with Ki-67. To compare the colocalization of rhinovirus with cycling cells, we used cell sheets at 10 days after confluence, because these would have more cycling cells than at 21 days, as applied in most of our studies. We used our standard 1-hour exposure to virus with a 24-hour period after exposure. Although we observed a significantly increased number of Ki-67–positive cells in IL-13–treated cell sheets (101 ± 7 Ki-67 per field versus 79 ± 7 Ki-67 per field in untreated cell sheets, $n = 8$ fields, three cultures; $P < 0.05$), no colocalization of Ki-67–positive cells and rhinovirus infection occurred (Figure 8). In addition, Ki-67–positive cells were primarily localized to the basal cell layers, whereas virus was located more apically. Therefore, enhanced levels of infection are not a result of the proliferative effects of IL-13.

We next asked whether the lower R_{te} of mucous cultures (1,536 ± 93 versus 966 ± 86 $\Omega \times cm^2$) was associated with higher levels of infection. The low R_{te} may have been attributable to breaks in tight junctions and increased access of virus to basolateral receptors. In mucociliary cells from these tracheas, R_{te} showed a fivefold range from 500 to 2,500 $\Omega \times cm^2$, but the linear regression of the percentage of infected cells per filter on R_{te} was not statistically significant ($R^2 = 0.001$, $P = 0.857$; $n = 24$ cell sheets from eight tracheas). In cells treated with IL-13, a wide range in R_{te} (400 to 1,600 $\Omega \times cm^2$) overlapped substantially with the R_{te} levels of mucociliary cultures. Again, no statistically significant dependence of numbers of infected cells on R_{te} was evident ($R^2 = 0.055$, $P = 0.231$; $n = 24$, eight tracheas).

As mentioned previously, the apical membranes of cells treated with IL-13 were larger and less ciliated than in untreated cultures, suggesting that the ability of cells to bind and internalize virus correlated with the flatness of their apical membranes. This hypothesis already receives considerable support from our earlier finding of greatly increased levels of infection in squamous cultures (9). However, in cultures grown under conditions that produce mucociliary differentiation, it is well-established that the complexity of the apical membrane increases progressively over the first 28 days in culture (10, 13).

TABLE 2. CELL COUNTS QUANTIFYING NUMBER OF CELLS POSITIVE FOR RHINOVIRUS BY IMMUNOFLUORESCENCE

	Control Cells	IL-13
Total number of infected cells	110 ± 7	281 ± 38*
Total number of infected goblet cells	59 ± 6	213 ± 33*
Total number of infected non–goblet cells	51 ± 9	68 ± 9

Data were collected from six mature cell sheets grown at an air–liquid interface with four randomly selected fields from each sheet. sheets were from each of two different tracheas. Data represent an average of 24 fields for each treatment group. Data were determined using antibody B6E8. Exactly comparable results were obtained with MUC5AC clone 45M1. *See* online supplement.

* Significantly different from control cells.

Therefore, cells from one trachea were exposed to virus at set times 10–32 days after confluence (cultures used in the other studies described here were all exposed to virus at 21 days). With increasing age, control cultures (untreated with IL-13) showed a progressive decline in numbers of infected cells, from ~2% at 10 days to ~0.1% at 32 days (Table 3). The decrease in levels of infection with time was statistically significant (best least squared linear regression, $R^2 = 0.767$; $n = 5$). In contrast, cells treated with IL-13 for 7-days before adding virus showed a significant increase ($R^2 = 0.776$) in levels of infection over the same period (Table 3).

DISCUSSION

Infection of airway epithelium by rhinovirus is the most common cause of asthma exacerbations. Even in mild asthma, airway epithelium shows mucous metaplasia, and the degree of this metaplasia increases with increasing severity of the disease. We previously showed that squamous cultures of human airway epithelium show levels of viral infection ~ 100-fold greater than those of mucociliary cultures derived from cells from the same trachea (9). Here, we further show that the change from the mucociliary to the mucous metaplasia phenotype is also associated with increased susceptibility to rhinoviral infection.

We induced mucous metaplasia with IL-13. Several lines of evidence suggest that this cytokine plays a major role in the induction of mucous metaplasia seen in asthma (26–29). IL-13 has been shown to increase in bronchial tissues from patients with asthma (30). The IL-13 treatment of primary cultures from human airway epithelium increases the ratio of secretory cells to ciliated cells, induces goblet-cell metaplasia, and decreases ciliary beat frequency, and these effects can be reversed by blocking the receptor to IL-13 (25, 26, 28, 31, 32). IL-13 is produced by most resident airway cells, with differential expression between cell types (33). IL-13 has been shown to play a direct role in propagating and perpetuating airway inflammation, initiating subepithelial fibrosis, regulating mucous hypersecretion, and causing alterations to epithelial cell function (34). Polymorphisms in the IL-13 gene have been linked to an increased incidence of, and susceptibility to asthma (35).

We found that treatment with 10 ng/ml IL-13 for 7 days increased the release of mucin, as measured by ELISA. Moreover, observable increases occurred in the number of cells that stained for either antibody B6E8 (Table 1 and Figure 1B) or FPAS (Figure 1A), or that appeared to be mucous cells by light

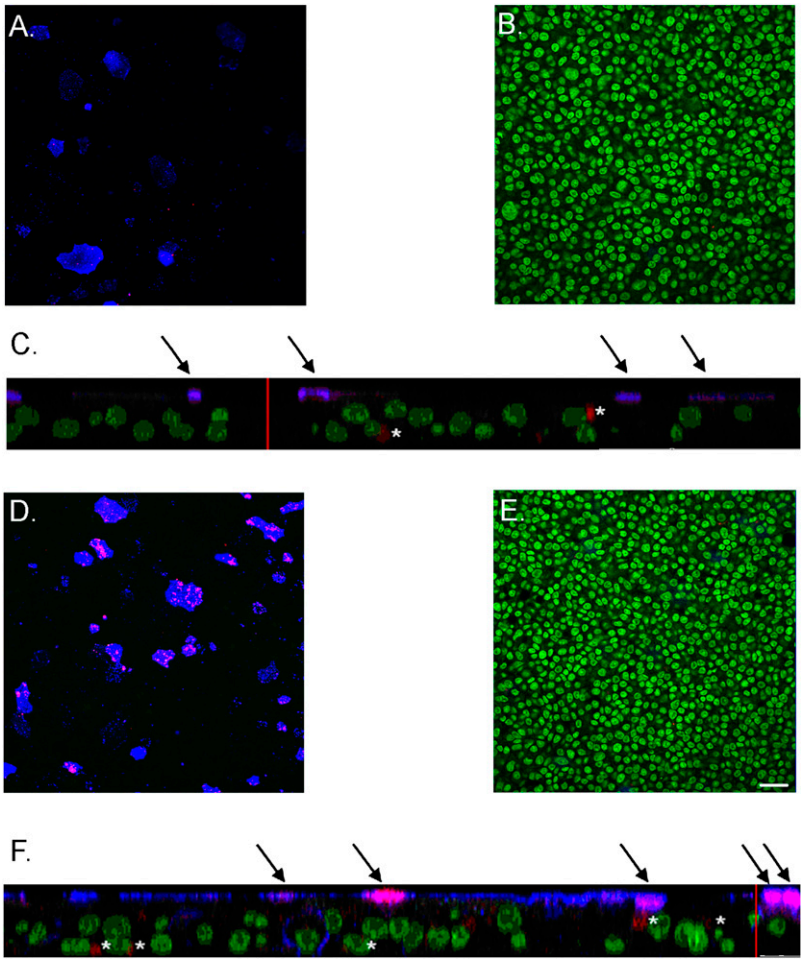

Figure 5. Rhinovirus preferentially infects goblet cells, an effect enhanced by goblet-cell metaplasia induced by IL-13. Nuclei, *green*; mucus, *blue*; virus, *red*. (*A*) Apical plane of control cell sheets shows colocalization of virus to goblet cells. (*B*) Center plane of control cell sheets shows no mucus staining. (C) Z-stack of control cell sheets. (*D*) Apical plane of IL-13–treated cell sheet shows colocalization of virus to goblet cells. (*E*) Center plane of IL-13–treated cell sheet shows no mucus staining. (*F*) Z-stack of IL-13–treated cell sheets; *scale bar* = 25 μm. *Arrows* indicate colocalization of mucus and virus. Where this occurs in IL-13–treated cells, levels of both mucus and virus are higher than in control cells. *Asterisks* indicate virus unassociated with mucus. Cells sheets were grown from the same trachea. *Scale bar* in E = 25 μm. Same scale for *A, B, D*, and *E*. *Red vertical bars* in z-stacks represent 25 μm.

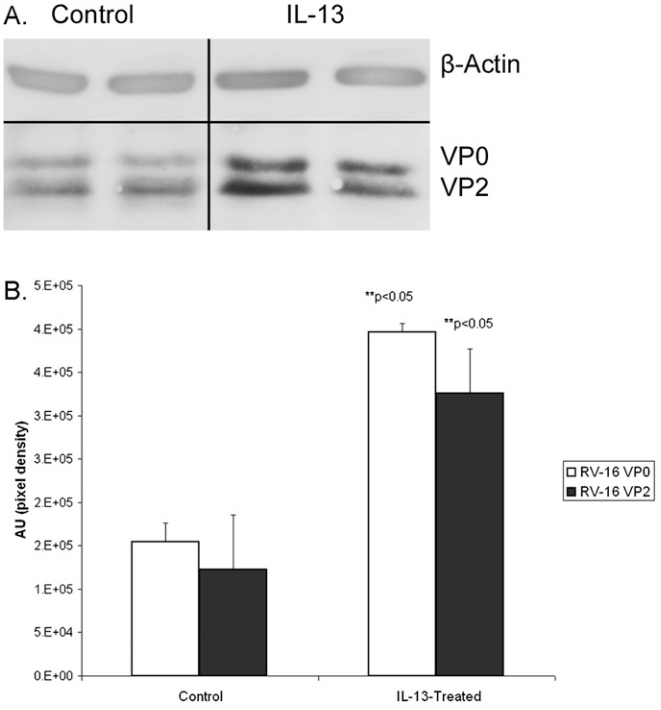

Figure 6. Quantification of rhinovirus infection by Western blot (*A*) IL-13–treated cell sheets have higher levels of rhinovirus capsid proteins, when normalized to β-actin levels. (*B*) Pooled data from three experiments. Rhinovirus proteins VP_2 and VP_0 are detected at ~3-fold higher levels in cell lysates from IL-13–treated cell sheets. *AU*, arbitrary units as a measure of pixel density.

microscopy (Figure 1C). The increase in the number of mucous cells was accompanied by a reduction in the degree of ciliation of cultures, with significantly decreased R_{te}. These results suggest that IL-13–treated cultures represent a good model for the epithelial phenotype of mucous hyperplasia and metaplasia associated with asthma.

The effects of IL-13 on susceptibility to rhinoviral infection appeared entirely attributable to the induction of mucous metaplasia. Thus, the increase in numbers of infected cells equaled the change in numbers of infected goblet cells. Furthermore, the odds of a given mucous cell being infected were increased by IL-13 treatment.

Further evidence that the effects of IL-13 on levels of viral infection were attributable to the induction of mucous metaplasia in mucociliary cultures was obtained by using squamous cultures. Pretreatment of these cultures with IL-13 caused no structural changes whatsoever. In particular, mucous cells did not appear, and levels of rhinoviral infection did not increase.

We investigated the hypothesis that the increased levels of rhinoviral infection seen with mucous metaplasia were attributable to increased levels of ICAM-1 on the apical membrane. Immunocytochemical staining for ICAM-1 was most intense on the apical membrane, with no overt differences in staining pattern or intensity between mucociliary and mucous cultures. Furthermore, total levels of ICAM-1, as determined by Western blotting, were identical in the two cell types (although squamous cells contained about four times more ICAM-1 than either). However, we acknowledge the need for caution in the interpretation of Western blots. Doubtless, ICAM-1 is densest on apical membranes, but the area of a basolateral membrane is greater, and ICAM-1 from this latter membrane (or from the cytoplasm) may make a greater contribution to total levels than anticipated from the immunocytochemical data. Interestingly, total levels of ICAM-1 in squamous cultures were ~ 4 times greater than in mucociliary cultures (Figure 7A), but the levels of virus produced were at least 100 times greater (9). This finding emphasizes the importance of factors other than binding sites in the total amount of virus produced by any epithelial phenotype.

Next, we tested the hypothesis that rhinovirus preferentially infected cycling or dividing cells. Many examples exist of both DNA and RNA viruses (36–39) that require host factors for translation and replication, and that replicate better in dividing than nondividing cells. However, we never observed a colocalization of Ki-67 and rhinovirus. We interpret this result to mean that dividing cells do not have apical membranes, and cannot be infected by rhinovirus. This interpretation is further validated by the finding that cycling cells were only found at the bottom layers of cell sheets in both treatment conditions.

A highly ciliated epithelium, as seen in healthy airways, may sterically block rhinovirus from accessing its receptor ICAM-1. Thus, we speculate that the ability of rhinovirus to bind to ICAM-1 and to be endocytosed is increased in cells with flatter apical surfaces. This would explain the very high levels of infection seen in squamous cultures (9). Consistent with this hypothesis, we found large apical membranes with reduced ciliation in IL-13–treated sheets. To test this idea further, we compared levels of infection in control cultures of different ages. Cultures after ~10 days showed no ciliation and no goblet cells, and possessed comparatively undifferentiated apical membranes (13). However, the levels of infection were at least four times greater than in cultures after $>$ 21 days, at which time mucociliary differentiation is well advanced (13, 40).

Ezrin is a key component in the clathrin-mediated internalization of rhinovirus (41). After a 12-day treatment of cultured spheroids from human tracheal epithelium with IL-13, levels of ezrin declined by 30% (25), although no change was evident after 7 days (the treatment duration used in the present studies). Furthermore, with the transition from a mucociliary to a mucous phenotype, the predominant ezrin staining shifted from the microvilli of ciliated cells to the cytoplasm, although the authors did not indicate whether ciliated or secretory cells were involved (25). Clearly, such changes in the levels and distribution of ezrin will affect the internalization of rhinovirus, and may be responsible for the increased uptake of virus seen with mucous metaplasia, or alternatively, may alter the effects of potentiating factors that potentiate viral replication.

The increase in the number of goblet cells in IL-13–treated sheets was accompanied by a decrease in R_{te}. We therefore considered the possibility that the increased levels of infection in mucous cultures compared with mucociliary cultures may be attributable to reduced barrier function. However, we reject this hypothesis for a number of reasons. First, we show here that in control cells and in cells treated with IL-13, there is no dependence of levels of infection on R_{te}. Second, in other work (Sachs and Widdicombe, unpublished findings), we exposed cells to Ca–Mg-free medium. This exposure opened tight junctions, as revealed by a decline in R_{te} to zero, but had no effect on the numbers of cells infected with virus. Third, the addition of virus to the basolateral side of the cultures produced levels of infection considerably lower than with additions to the apical surface (Sachs and Widdicombe, unpublished findings). This is consistent with our immunocytochemical finding that ICAM-1 has a predominantly apical localization (Figure 7C). Fourth, we find little reason to believe that pores the size of rhinoviruses exist in airway epithelium in general or in our cultures in particular. Multiple images from both scanning electron microscopy and confocal fluorescence microscopy showed that our cultures, regardless of resistance, were all

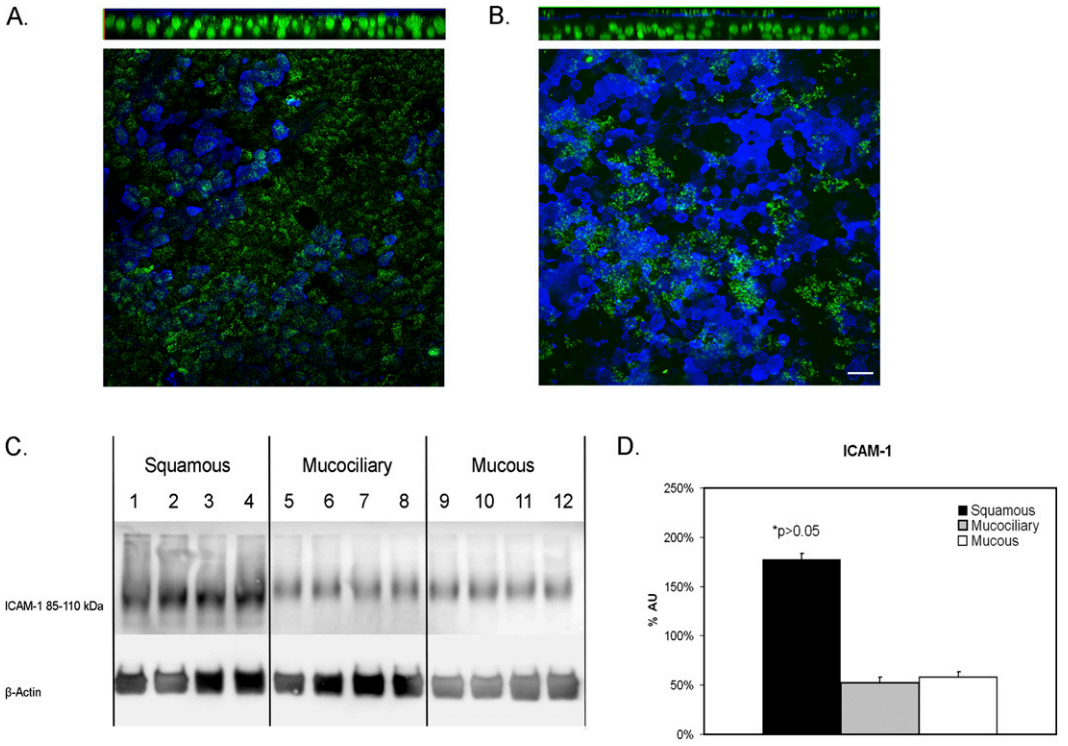

Figure 7. Quantification of rhinovirus receptor ICAM-1 in airway epithelial cells. (*A*) Immunofluorescence of ICAM-1 in control cell sheets shows the receptor is primarily localized to the apical surface. (*B*) Immunofluorescence of ICAM-1 in IL-13–treated cell sheets shows similar apical localization of ICAM-1, with no apparent association with goblet-cell staining. *Top*: Z-projection of an x–y stack. *Bottom*: x–y plane at level of the apical membrane. B6E8, *blue*; ICAM-1, *green*, at apical membrane; nuclei, *green*, using Yo-Pro-1. *Scale bar* = 15 μm. (*C*) Squamous-cell sheets have higher levels of ICAM-1 protein levels, compared with control cell sheets when normalized to β-actin levels. Mucus (IL-13–treated) and mucociliary cell sheets have similar levels of ICAM-1 protein when normalized to β-actin levels. (*D*) Pooled data from three experiments. AU, arbitrary units as a measure of pixel density.

completely confluent. No gaps were visible in the cell sheet, and ZO-1 staining revealed that every cell was surrounded by an intact tight junction. Hence virus would have to penetrate through tight junctions, and the effective pore size of even the leakiest of these is ~4 Å (42, 43) Tricellular junctions, i.e., the points where tight junctions branch, constitute an exception to this statement. But even here, the effective pore diameter was estimated as ~ 10 nm at most (44), although functional studies indicate that it is usually much less (45).

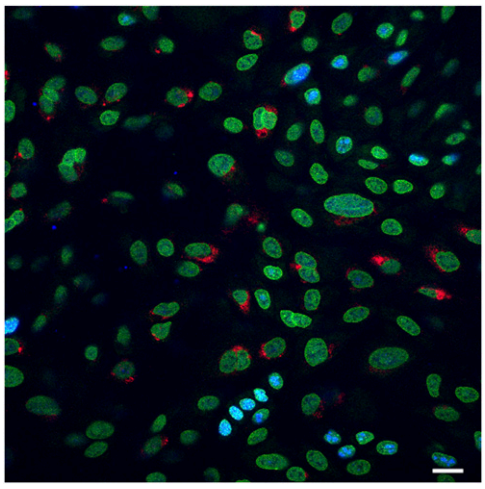

Figure 8. Immunofluorescence of Ki-67 (*blue*) and rhinovirus (*red*) shows no correlation between dividing cells and infection. Nuclei are *green*. Results are from a 10-day-old culture in which division was greater than at 21 days. However, virus only infected nondividing cells at all ages. *Scale bar* = 10 μm.

Our viral preparation was a crude cell lysate, and thus the increased level of viral infection seen in mucous cells may be attributable to a selective action of these contaminants on this cell type. Unfortunately, such an effect can never be ruled out completely, because eliminating contaminants entirely is impossible. Thus, concentrating a virus with centrifugal filters or similar devices will merely enhance the concentration of virus relative to contaminants. Key contaminants may still be present in the suspension at concentrations supramaximal for the observed effect. However, we think a selective action of contaminants is unlikely for three reasons. First, exposure times to virus were brief (1 hour), thereby minimizing the time available for any contaminants to induce significant changes in the cellular apparatus for the binding and internalization of virus. Second, viral suspension was added to the mucosal surface of confluent cell sheets, and epithelial receptors for cytokines and other bioactive agents are generally on the basolateral membrane. Third, we used virus at a concentration of 10^5 $TCID_{50}$/ml, a 63-fold dilution of the original suspension ($10^{6.8}$ $TCID_{50}$/ml).

We show that mucous metaplasia *in vitro* is associated with increased levels of viral infection. Even patients with mild

TABLE 3. DEPENDENCE OF INFECTION ON AGE OF CULTURE

Culture	Age (Days)	Control Cells (Percentage of Cells Infected)	IL-13 (Percentage of Cells Infected)
A	10	1.76 ± 0.35	2.33 ± 0.45
B	12	1.40 ± 0.13	2.72 ± 0.20
C	14	0.69 ± 0.03	3.28 ± 0.04
D	21	0.48 ± 0.03	6.52 ± 0.08
E	32	0.13 ± 0.01	6.27 ± 0.05

Data are from four randomly selected fields from each of two cell sheets per age. IL-13 was added 7 days before adding virus.

asthma have more goblet cells in their airway epithelium. Moreover, consistent with higher levels of viral infection, patients with asthma contract abnormally severe lower respiratory tract symptoms during colds (46, 47). Therefore, during a cold, patients with asthma should demonstrate more shedding of virus from the epithelium. However, studies involving experimental inoculations of rhinovirus failed to show an effect of asthma on viral titers in nasal lavages or induced sputum (48). Several reasons for this discrepancy between *in vivo* and *in vitro* studies are possible. First, most patients in studies of experimental inoculations *in vivo* have comparatively mild asthma, and therefore presumably less mucous metaplasia than with *in vitro* systems. Second, comparisons of viral release from patients with asthma and normal subjects *in vivo* are made difficult by the extreme variability in levels of virus recovered. For instance, in a study by Message and colleagues (47), viral titers in nasal lavage or induced sputum varied over at least five orders of magnitude, and although virus retrieved in lavages or sputum from patients with asthma averaged from 0.5–2 logs greater than normal, these differences were not statistically significant. Finally, however good the culture model, the possibility always remains that results obtained *in vitro* do not apply to the more complex situation *in vivo*.

In conclusion, our study shows that mucous metaplasia increases the susceptibility of the airway epithelium to rhinovirus infection. Furthermore, our data suggest that the increased susceptibility is attributable to a loss of apical membrane complexity. We induced mucous metaplasia with IL-13, and this agent may also be largely responsible for the mucous metaplasia of airway epithelium in asthma. Our results therefore have important implications concerning IL-13 as a target for asthma therapy. Most of the costs, and most of the morbidity, of asthma are attributable to asthma exacerbations, and most exacerbations are triggered by viral respiratory infections (49, 50), and especially by rhinovirus. A recent study described the association of increased levels of serum IL-13 with rhinovirus-induced asthmatic symptoms (47). Allergen ovalbumin (OVA)-challenged mice infected with rhinovirus also have increased levels of serum IL-13 (51). Therefore, blockade of IL-13 may inhibit the mucous metaplasia often associated with asthma (52), and by so doing may reduce the frequency and severity of asthma exacerbations.

Author Disclosure: H.A.B. received a research grant for more than $100,000 from GlaxoSmithKline. None of the other authors has a financial relationship with a commercial entity that has an interest in the subject of this manuscript.

Acknowledgments: We thank Lorne Sachs for technical assistance.

References

1. van Elden LJR, Sachs APE, van Loon AM, Haarman M, van de Vijver DA, Kimman TG, Zuithoff P, Schipper PJ, Verheij TJM, Nijhuis M. Enhanced severity of virus associated lower respiratory tract disease in asthma patients may not be associated with delayed viral clearance and increased viral load in the upper respiratory tract. *J Clin Virol* 41(2):116–121.
2. Papadopoulos NG, Papi A, Psarras S, Johnston SL. Mechanisms of rhinovirus-induced asthma. *Paediatr Respir Rev* 2004;5:255–260.
3. Jackson DJ, Gangnon RE, Evans MD, Roberg KA, Anderson EL, Pappas TE, Printz MC, Lee W-M, Shult PA, Reisdorf E, *et al.* Wheezing rhinovirus illnesses in early life predict asthma development in high risk children. *Am J Respir Crit Care Med* 2008;178:667–672.
4. Hansbro NG, Horvat JC, Wark PA, Hansbro PM. Understanding the mechanisms of viral induced asthma: new therapeutic directions. *Pharmacol Ther* 2008;117:313–353.
5. Tan WC. Viruses in asthma exacerbations. *Curr Opin Pulm Med* 2005; 11:21–26.
6. Cohen LEX, Tarsi J, Ramkumar T, Horiuchi TK, Cochran R, DeMartino S, Schechtman KB, Hussain I, Holtzman MJ, *et al.* Epithelial cell proliferation contributes to airway remodeling in severe asthma. *Am J Respir Crit Care Med* 2007;176:138–145.
7. Woodruff PMD, Fahy JMD. Airway remodeling in asthma. *Semin Respir Crit Care Med* 2002;23:361–368.
8. Fahy JV. Remodeling of the airway epithelium in asthma. *Am J Respir Crit Care Med* 2001;164:S46–S51.
9. Lopez-Souza N, Dolganov G, Dubin R, Sachs LA, Sassina L, Sporer H, Yagi S, Schnurr D, Boushey HA, Widdicombe JH. Resistance of differentiated human airway epithelium to infection by rhinovirus. *Am J Physiol Lung Cell Mol Physiol* 2004;286:L373–L381.
10. Yamaya M, Finkbeiner WE, Chun SY, Widdicombe JH. Differentiated structure and function of cultures from human tracheal epithelium. *Am J Physiol Lung Cell Mol Physiol* 1992;262:L713–L724.
11. Sachs L, Finkbeiner W, Widdicombe J. Effects of media on differentiation of cultured human tracheal epithelium. *In Vitro Cell Dev Biol Anim* 2003;39:56–62.
12. Widdicombe J, Sachs L, Finkbeiner W. Effects of growth surface on differentiation of cultures of human tracheal epithelium. *In Vitro Cell Dev Biol Anim* 2003;39:51–55.
13. LeDizet M, Beck JC, Finkbeiner WE. Differential regulation of centrin genes during ciliogenesis in human tracheal epithelial cells. *Am J Physiol Lung Cell Mol Physiol* 1998;275:L1145–L1156.
14. Tanabe T, Fujimoto K, Yasuo M, Tsushima K, Yoshida K, Ise H, Yamaya M. Modulation of mucus production by interleukin-13 receptor alpha2 in the human airway epithelium. *Clin Exp Allergy* 2008; 38:122–134.
15. Zhen G, Park SW, Nguyenvu LT, Rodriguez MW, Barbeau R, Paquet AC, Erle DJ. IL-13 and epidermal growth factor receptor have critical but distinct roles in epithelial cell mucin production. *Am J Respir Cell Mol Biol* 2007;36:244–253.
16. Skowron-zwarg M, Boland S, Caruso N, Coraux C, Marano F, Tournier F. Interleukin-13 interferes with CFTR and AQP5 expression and localization during human airway epithelial cell differentiation. *Exp Cell Res* 2007;313:2695–2702.
17. Lin HCD, St George JA, Plopper CG, Wu R. An ELISA method for quantitation of tracheal mucins from human and nonhuman primates. *Am J Physiol Lung Cell Mol Physiol* 1989;1:41–48.
18. Ino H. Application of antigen retrieval by heating for double-label fluorescent immunohistochemistry with identical species-derived primary antibodies. *J Histochem Cytochem* 2004;52:1209–1217.
19. Mosser A, Brockman-Schneider R, Amineva S, Burchell L, Sedgwick J, Busse W, Gern J. Similar frequency of rhinovirus infectible cells in upper and lower airway epithelium. *J Infect Dis* 2002;185:734–743.
20. Finkbeiner WE, Basbaum CB. Monoclonal antibodies directed against human airway secretions. Localization and characterization of antigens. *Am J Pathol* 1988;131:290–297.
21. Laoukili J, Perret E, Middendorp S, Houcine O, Guennou C, Marano F, Bornens M, Tournier F. Differential expression and cellular distribution of centrin isoforms during human ciliated cell differentiation *in vitro*. *J Cell Sci* 2000;113:1355–1364.
22. Kiesslich R, Goetz M, Angus EM, Hu Q, Guan Y, Potten C, Allen T, Neurath MF, Shroyer NF, Montrose MH, *et al.* Identification of epithelial gaps in human small and large intestine by confocal endomicroscopy. *Gastroenterology* 2007;133:1769–1778.
23. Tyler WS, Dungworth DL, Plopper CG, Hyde DM, Tyler NK. Structural evaluation of the respiratory system. *Fundam Appl Toxicol* 1985;5: 405–422.
24. Gomperts BN, Kim LJ, Flaherty SA, Hackett BP. IL-13 regulates cilia loss and foxj1 expression in human airway epithelium. *Am J Respir Cell Mol Biol* 2007;37:339–346.
25. Laoukili J, Perret E, Willems T, Minty A, Parthoens E, Houcine O, Coste A, Jorissen M, Marano F, Caput D, *et al.* IL-13 alters mucociliary differentiation and ciliary beating of human respiratory epithelial cells. *J Clin Invest* 2001;108:1817–1824.
26. Kondo M, Tamaoki J, Takeyama K, Nakata J, Nagai A. Interleukin-13 induces goblet cell differentiation in primary cell culture from guinea pig tracheal epithelium. *Am J Respir Cell Mol Biol* 2002;27:536–541.
27. Doherty T, Broide D. Cytokines and growth factors in airway remodeling in asthma. *Curr Opin Immunol* 2007;19:676–680.
28. Kondo M, Tamaoki J, Takeyama K, Isono K, Kawatani K, Izumo T, Nagai A. Elimination of IL-13 reverses established goblet cell metaplasia into ciliated epithelia in airway epithelial cell culture. *Allergol Int* 2006;55:329–336.
29. Fulkerson PC, Fischetti CA, Hassman LM, Nikolaidis NM, Rothenberg ME. Persistent effects induced by IL-13 in the lung. *Am J Respir Cell Mol Biol* 2006;35:337–346.
30. Huang SK, Xiao HQ, Kleine-Tebbe J, Paciotti G, Marsh DG, Lichtenstein LM, Liu MC. IL-13 expression at the sites of

allergen challenge in patients with asthma. *J Immunol* 1995;155: 2688–2694.
31. Yasuo M, Fujimoto K, Tanabe T, Yaegashi H, Tsushima K, Takasuna K, Koike T, Yamaya M, Nikaido T. Relationship between calcium-activated chloride channel 1 and MUC5AC in goblet cell hyperplasia induced by interleukin-13 in human bronchial epithelial cells. *Respiration* 2006;73:347–359.
32. Yoshisue H, Hasegawa K. Effect of MMP/ADAM inhibitors on goblet cell hyperplasia in cultured human bronchial epithelial cells. *Biosci Biotechnol Biochem* 2004;68:2024–2031.
33. Lee JH, Kaminski N, Dolganov G, Grunig G, Koth L, Solomon C, Erle DJ, Sheppard D. Interleukin-13 induces dramatically different transcriptional programs in three human airway cell types. *Am J Respir Cell Mol Biol* 2001;25:474–485.
34. Wills-Karp M. Interleukin-13 in asthma pathogenesis. *Immunol Rev* 2004;202:175–190.
35. Cameron L, Webster RB, Strempel JM, Kiesler P, Kabesch M, Ramachandran H, Yu L, Stern DA, Graves PE, Lohman IC, *et al.* Th2 cell-selective enhancement of human IL13 transcription by IL13–1112C>T, a polymorphism associated with allergic inflammation. *J Immunol* 2006;177:8633–8642.
36. Gamarnik AV, Boddeker N, Andino R. Translation and replication of human rhinovirus type 14 and mengovirus in *Xenopus* oocytes. *J Virol* 2000;74:11983–11987.
37. Schang LM. The cell cycle, cyclin-dependent kinases, and viral infections: new horizons and unexpected connections. *Prog Cell Cycle Res* 2003;5:103–124.
38. Gamarnik AV, Andino R. Replication of poliovirus in *Xenopus* oocytes requires two human factors. *EMBO J* 1996;15:5988–5998.
39. Feuer R, Mena I, Pagarigan R, Slifka MK, Whitton JL. Cell cycle status affects coxsackievirus replication, persistence, and reactivation in vitro. *J Virol* 2002;76:4430–4440.
40. Ross AJ, Dailey LA, Brighton LE, Devlin RB. Transcriptional profiling of mucociliary differentiation in human airway epithelial cells. *Am J Respir Cell Mol Biol* 2007;37:169–185.
41. Lau C, Wang X, Song L, North M, Wiehler S, Proud D, Chow C-W. SYK associates with clathrin and mediates phosphatidylinositol 3-kinase activation during human rhinovirus internalization. *J Immunol* 2008; 180:870–880.
42. Diamond JM. Twenty-first Bowditch lecture. The epithelial junction: bridge, gate, and fence. *Physiologist* 1977;20:10–18.
43. Van Itallie CM, Anderson JM. Claudins and epithelial paracellular transport. *Annu Rev Physiol* 2006;68:403–429.
44. Staehelin LA. Further observations on the fine structure of freeze-cleaved tight junctions. *J Cell Sci* 1973;13:763–786.
45. Krug SM, Amasheh S, Richter JF, Milatz S, Gunzel D, Westphal JK, Huber O, Schulzke JD, Fromm M. Tricellulin forms a barrier to macromolecules in tricellular tight junctions without affecting ion permeability. *Mol Biol Cell* 2009;20:3713–3724.
46. Corne JM, Marshall C, Smith S, Schreiber J, Sanderson G, Holgate ST, Johnston SL. Frequency, severity, and duration of rhinovirus infections in asthmatic and non-asthmatic individuals: a longitudinal cohort study. *Lancet* 2002;359:831–834.
47. Message SD, Laza-Stanca V, Mallia P, Parker HL, Zhu J, Kebadze T, Contoli M, Sanderson G, Kon OM, Papi A, *et al.* Rhinovirus-induced lower respiratory illness is increased in asthma and related to virus load and Th1/2 cytokine and IL-10 production. *Proc Natl Acad Sci USA* 2008;105:13562–13567.
48. Bardin PG, Fraenkel DJ, Sanderson G, van Schalkwyk EM, Holgate ST, Johnston SL. Peak expiratory flow changes during experimental rhinovirus infection. *Eur Respir J* 2000;16:980–985.
49. Smith DH, Malone DC, Lawson KA, Okamoto LJ, Battista C, Saunders WB. A national estimate of the economic costs of asthma. *Am J Respir Crit Care Med* 1997;156:787–793.
50. Weiss KB, Sullivan SD. The health economics of asthma and rhinitis. I. Assessing the economic impact. *J Allergy Clin Immunol* 2001;107: 3–8.
51. Bartlett NW, Walton RP, Edwards MR, Aniscenko J, Caramori G, Zhu J, Glanville N, Choy KJ, Jourdan P, Burnet J, *et al.* Mouse models of rhinovirus-induced disease and exacerbation of allergic airway inflammation. *Nat Med* 2008;14:199–204.
52. Rogers DF, Barnes PJ. Treatment of airway mucus hypersecretion. *Ann Med* 2006;38:116–125.